

IBM Research Report

Flow Box Tiling Methods for Compact Invariant Manifolds

Michael E. Henderson
IBM Research Division
Thomas J. Watson Research Center
P.O. Box 218
Yorktown Heights, NY 10598



Research Division

Almaden - Austin - Beijing - Cambridge - Haifa - India - T. J. Watson - Tokyo - Zurich

FLOW BOX TILING METHODS FOR COMPACT INVARIANT MANIFOLDS

MICHAEL E. HENDERSON[†]

Abstract. Invariant manifolds are important to the study of the qualitative behavior of dynamical systems and nonlinear control. Good algorithms exist for finding many one dimensional invariant curves, such as periodic orbits, orbits connecting fixed points, and more recently two dimensional stable and unstable manifolds of fixed points. This paper addresses the problem of computing higher dimensional closed invariant manifolds, for example invariant tori, using an approach that produces a large system of coupled two point boundary value problems.

The algorithm described here is not limited to a particular dimension or topology. It does not assume that a closed global section exists, nor that a splitting or parameterization of the manifold is known a priori. A flow box tiling is used to construct a set of trajectory fragments on the manifold which are used to pose a system of coupled two point boundary value problems for the manifold.

1. Introduction. Invariant manifolds are important to the study of the qualitative behavior of dynamical systems and nonlinear control. Good algorithms exist for finding many one dimensional invariant curves, such as periodic orbits [6], [14], orbits connecting fixed points [18], [11], and more recently two dimensional stable and unstable manifolds of fixed points and periodic orbits [25].

A Closed Connected Invariant Manifold $M(\lambda)$ *is a compact connected manifold with no boundary embedded in \mathbb{R}^n which is invariant under a parameter dependant flow $\mathbf{f}(\mathbf{u}, \lambda)$. That is, if*

$$\begin{aligned} \mathbf{u} \in \mathbb{R}^n, \quad \lambda \in \mathbb{R}^p \quad \mathbf{f} : \mathbb{R}^n \times \mathbb{R}^p \rightarrow \mathbb{R}^n \\ \mathbf{u}(0) \in M(\lambda), \quad \text{and} \quad \mathbf{u}'(t) = \mathbf{f}(\mathbf{u}(t), \lambda), \end{aligned}$$

then

$$\mathbf{u}(t) \in M(\lambda) \quad \text{for all } t \in (-\infty, \infty).$$

Except in the case where M is the level set of an integral of the system (e.g. in Hamiltonian systems), $M(\lambda)$ will not persist in a neighborhood of λ unless it is normally hyperbolic [17], [22]. We will assume that this is the case throughout.

In many practical cases the embedding space will be high dimensional, and so we will try to avoid using the normal space of the manifold.

Numerical methods for computing periodic orbits use a Poincaré Section. Near the periodic orbit trajectories cross the section transversally, and trajectories which begin on the section return to the section. This approach has been applied to quasiperiodic tori (Sec. 2), but only certain topologies of M and certain flows on those topologies have such closed transverse sections, and corresponding smooth return maps.

The algorithm described below uses a flowbox tiling to construct a different type of section, which does not assume a particular topology of the manifold, and applies to a broad range of topologies and dimensions greater than two. (Sec. 3). The

[†]IBM Research Division, T. J. Watson Research Center, Yorktown Heights, NY 10598, mhender@watson.ibm.com

return map on this generalization is piecewise smooth, and will be approximated by a large system of coupled two point boundary value problems (TPBVPs) (Sec. 4). The coupling is not the usual coupling through boundary conditions, but involves interior values. Solvers for this type of system of TPBVP's do not exist at present, but require a fairly straightforward modification of existing techniques. These modifications have not yet been implemented, so we can show the initial flow box covering, and the system of TPBVP's, but not yet a solution of the system.

The parameter dependence is included so that this algorithm may be used with continuation methods [2] and [19] (and others). These methods assume that for some λ , $M(\lambda)$ is known. This initial manifold is then used to compute $M(\cdot)$ at a nearby value of λ . The process is repeated, eventually finding $M(\cdot)$ for $\lambda \in \Omega \subset \mathbb{R}^p$, some finite subset of parameter space.

There are several challenges involved in formulating a system for a closed invariant manifold. There is the size and structure of the linear systems which appear, the problem of constructing an adequate mesh, and the usual concerns of consistency and stability, which [28] rightly highlight.

2. Background. There are several ways to write a set of equations defining a closed invariant manifold. Below we briefly discuss three formulations and corresponding numerical methods which are based on them. Excellent discussions of the computational techniques are included in [28] and [30], and [33] provides a very good background of the theoretical results. We summarize the computational methods here so that similarities between existing approaches and the algorithm proposed here can be appreciated.

2.1. The Hadamard graph transform. If $\phi(\mathbf{u}, t)$ is the integral of the flow:

$$\frac{\partial}{\partial t} \phi(\mathbf{u}, t) = \mathbf{f}(\mathbf{u})$$

or

$$\phi(\mathbf{u}(0), t) = \mathbf{u}(0) + \int_0^t \mathbf{f}(\phi(\mathbf{u}(0), \tau)) d\tau,$$

then for any t ,

$$(2.1) \quad M = \phi(M, t).$$

Graph transform methods assume that M can be expressed as a graph over some domain U :

$$\mathbf{u} \in M \quad \Leftrightarrow \quad \mathbf{u} = \mathbf{g}(\mathbf{s}), \quad \mathbf{s} \in U.$$

Eq. 2.1 becomes

$$(2.2) \quad \mathbf{g}(\mathbf{s}(t)) = \phi(\mathbf{g}(\mathbf{s}(0)), t),$$

where $\mathbf{s}(t)$ is the integral of the flow projected onto U . Since M is a manifold it is represented as a set of graphs (charts), and the argument can be extended when more M consists of more than one chart.

If the invariant manifold is hyperbolic, then a contracting map can be constructed from Eq. 2.2 with M as a fixed point. If M is an attractor, and a graph \mathbf{g}_0 can be found in the basin of attraction of M , then letting t become large gives (Fig. 2.3).

$$(2.3) \quad \text{as } t \rightarrow \infty \quad \mathbf{g}(\mathbf{s}(t)) \rightarrow \phi(\mathbf{g}_0(\mathbf{s}(0)), t).$$

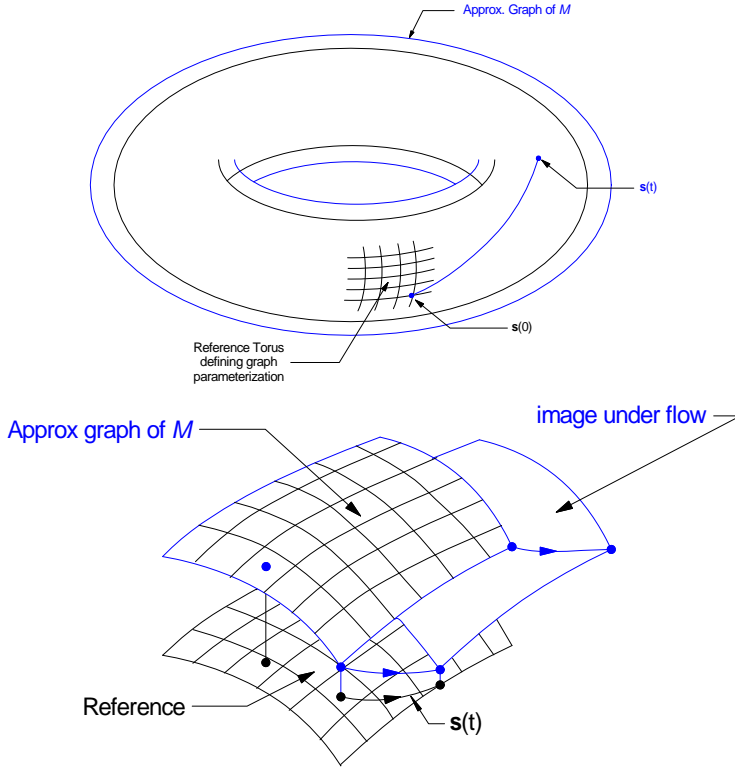


FIG. 2.1. An invariant torus used to parameterize inner and outer surfaces which converge to an invariant surface under the flow.

When M is normally hyperbolic but not an attractor this approach can be modified by splitting Eq. 2.2 local to $\mathbf{g}(\mathbf{s}(t))$ into the stable and unstable directions orthogonal to M . Eq. 2.3 can also be reformulated as a map by integrating over some small interval in time [29]. Or the integrated form can be solved using a Newton method [27], [9].

The main issue for these methods (apart from performing the splitting) is the distortion of the initial parameterization of \mathbf{g} . The distortion is the mapping $\mathbf{s}(t)$, and can be removed by reparameterizing \mathbf{g} after an iteration.

2.2. The PDE formulation. The differential form of Eq. 2.2 is

$$(2.4) \quad \frac{\partial \mathbf{g}}{\partial \mathbf{s}} \frac{\partial \mathbf{s}}{\partial t} = \frac{\partial \phi}{\partial \mathbf{t}} \quad \text{or,} \quad \mathbf{f}(\mathbf{u}) = \mathbf{u}_s \mathbf{s}'$$

where \mathbf{s}' is the flow \mathbf{f} projected on the tangent space of M . (see Fig. 2.2). The columns of the matrix $\mathbf{u}_s \equiv \Phi(\mathbf{u}(\mathbf{s}))$ span the tangent space of M at $\mathbf{u}(\mathbf{s})$. We use this notation $\Phi(\mathbf{u})$ rather than the more usual $T_{\mathbf{u}}(M)$ or $TM_{\mathbf{u}}$ to avoid confusion with subscripts used for differentiation. The function $\mathbf{s}'(t)$ may be eliminated using “orthogonal projections” [26]

$$(2.5) \quad (I - \Phi(\mathbf{u})\Phi^T(\mathbf{u})) \mathbf{f}(\mathbf{u}) = 0.$$

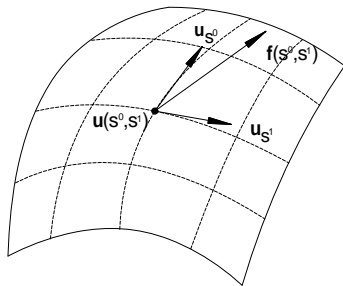


FIG. 2.2. An invariant surface. The PDE formulation requires that everywhere on the surface the flow direction lies in the tangent space of the surface.

If there is a splitting which makes the parameterization explicit, $\mathbf{u} = (\mathbf{r}, \theta)$ with

$$\mathbf{r}' = \mathbf{g}(\mathbf{r}(\theta), \theta)$$

$$\theta' = \mathbf{f}(\mathbf{r}(\theta), \theta),$$

then instead of $\Phi^T(\mathbf{u})(\mathbf{u} - \mathbf{u}_0) = 0$ we can use $\theta = \theta_0$ to parameterize M , and since $\mathbf{r}' = \mathbf{r}_\theta \theta'$, Eq. 2.4 becomes

$$(2.6) \quad \frac{\partial \mathbf{r}}{\partial \theta} \mathbf{f}(\mathbf{r}(\theta), \theta) = \mathbf{g}(\mathbf{r}(\theta), \theta).$$

Meshing the manifold is non-trivial, and the locally hyperbolic nature (in the sense of PDEs) of the equations can lead to instabilities orthogonal to the manifold [28]. Methods also vary somewhat in the parameterizations used normal and tangential to the manifold. A common approach is to use a reference manifold (for example $M(\lambda - \Delta\lambda)$):

$$(2.7) \quad \begin{aligned} \mathbf{f}(\mathbf{u}) &= \Phi(\mathbf{u})\alpha(\mathbf{u}) \\ \Phi^T(\mathbf{u})(\mathbf{u} - \mathbf{u}_0) &= 0 \end{aligned}$$

This uses the reference manifold to induce the parameterization of the unknown manifold. Schilder, Osinga and Vogt [30] consider quasiperiodic tori, for which $\alpha(\mathbf{u})$ is constant and is the vector of frequencies. For invariant tori the PDE can be posed a square with periodic boundary conditions.

2.3. Methods which find an invariant curve of a return map. Periodic orbits are closed invariant curves, and the computational approach used [15] (and others) is based on the Poincaré section Σ . This is a co-dimension one surface which the periodic curve crosses transversally, and which exists in some neighborhood of that intersection point. The integral of the flow then produces a map from Σ to itself, for which the periodic is a fixed point. This is equivalent to integrating the PDE formulation above in the time direction to obtain the return map (since there is only one trajectory it is hardly a PDE).

The generalization of the Poincaré section is a transverse section [24] pp. 53–55 and [23] pp. 55–58) (sometimes called a Poincaré surface of section [7]).

A Transverse Section is a set of codimension one surfaces on M none of which is tangent to the flow.

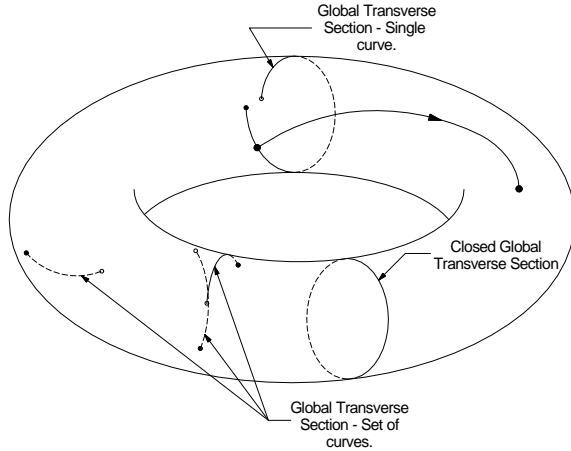


FIG. 2.3. A torus with three types global transversals. One is and open arc, one is a closed curve, and one is a set of open arcs. Any point on the torus is connected to a point on the section by a trajectory.

A Global Transverse Section is a transverse section such that every point on M lies on a trajectory passing through a point on the transverse section. (Fig. 2.3.)

The Poincaré section for a periodic orbit is a transverse section. The point of intersection of the section with the periodic orbit is a global transverse section for the flow on the orbit.

In cases where a global transverse section Σ exists on M a return map may be defined by integrating the section forward with the flow. Each point on the section may require a different integration time, which we will call $\tau(\xi)$, where ξ is a parameterization of the extension of Σ normal to M (Fig. 2.4). If the global section is $\xi(\mathbf{s})$, the return map is

$$(2.8) \quad \xi(\sigma(\mathbf{s})) = \phi(\xi(\mathbf{s}), \tau(\xi(\mathbf{s}))).$$

This approach is used by van Veldhuizen [32] for quasiperiodic tori (where a global section does indeed exist). The return map does not return mesh points to mesh points (Fig. 2.5, ($\sigma(\mathbf{s}_i) \neq \mathbf{s}_j$)) so an interpolation is needed.

3. Flow box tiling methods. The three approaches described above share many features. We have already pointed out that the PDE formulation is the differential version of the graph transform. The PDE formulation solves a hyperbolic system, whose characteristics are trajectories. Without reparameterizing the $\mathbf{s}(t)$ are trajectories, and each mesh point in the approximation of the graph moves along a trajectory on M . Now, if the system is integrated along the characteristics, each is an initial value problem. M is assumed to be compact, so each characteristic will return near to either itself or another characteristic. In the case of quasiperiodic tori, and when there is a global transversal, the return of the characteristics becomes a return map, and the characteristics may be chosen to begin and end on an invariant curve of the return map.

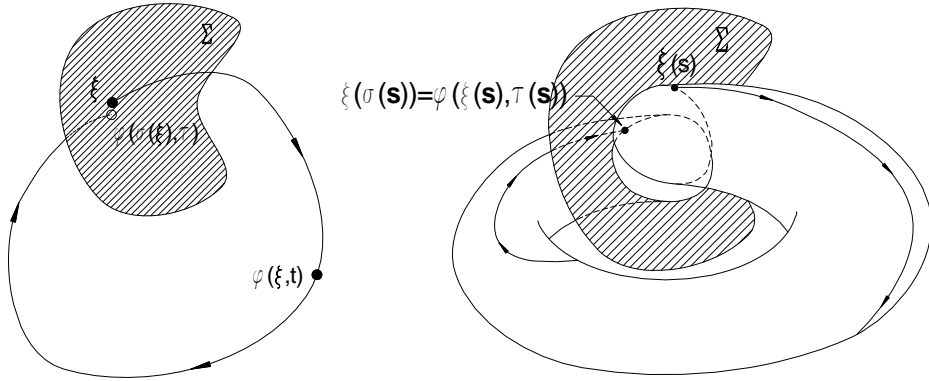


FIG. 2.4. Two transverse sections *l*) The return map has a single fixed point. The invariant manifold is a closed curve, and the intersection of the curve with the transverse section (a point) is a global transverse section for the invariant curve. *r*) The return map has an invariant circle. The invariant manifold is a torus, and the intersection of the torus with the section (a closed curve) is a closed global transverse for the invariant torus.

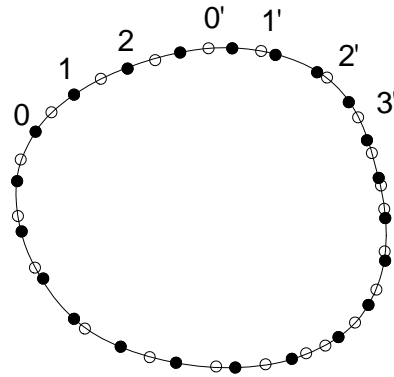


FIG. 2.5. A invariane circle and a set of points $(0, 1, 2, \dots)$ and their image under the map $(0', 1', 2', \dots)$. This mismatch is the result of the function $\sigma(\cdot)$ in Eq. 2.8, and means that an interpolation must be done.

From a computational viewpoint meshing is simplest for the PDE formulation, since mesh lines need not be related at all to the characteristics. For the integrated version of the graph transform, and the invariant curve approaches some reparameterization is necessary. This is an adaptive mesh problem, and can be problematic.

The algorithm proposed below incorporates various features of the three approaches. It produces a nonuniform mesh which locally has mesh lines which are trajectories. However, it allows the mesh to change, and so avoid the reparameterization problem. Secondly, in the linear algebra which results from implementing Newton's method on this mesh has a structure which allows elimination along the trajetries. This is similar to integrating trajectories to build a return map, but is done only in the solution of the linear system. equations along the charateristics of the PDE (trajectories).

3.1. Flow box coverings, tilings, and global sections which are sets of disks. The formulation of a quasiperiodic torus as an invariant circle of a map does

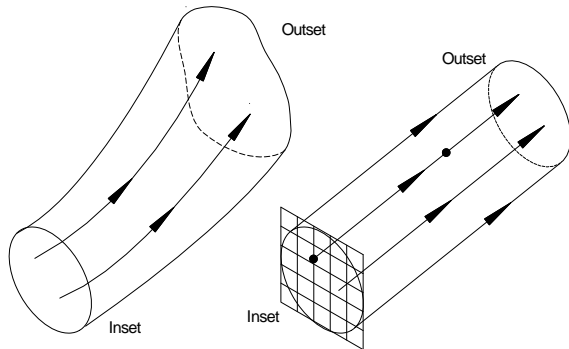


FIG. 3.1. A flow box. The inset is mapped to the outset under the flow. (left) Original coordinates. (right) The “straightened” flow box, using a coordinate system on the inset and time.

not easily apply to other flows on the torus, or to closed invariant manifolds with different topologies. Reeb flow on a torus [24], for example, does not have a closed global transversal. The existence of closed global transversals is intimately related to the topology of M and the flow [24]. In general it is not expected that a flow on a closed manifold has a closed global transversal. The formulation described below is based on finding invariant curves on a different kind of global transverse section, which exists in a larger class of problems, and is constructed from a flow box tiling of M [5]. The section exists whenever M can be covered by flow boxes, which holds if there is a flow box neighborhood of each point on M . This is trivially true when M contains no fixed points. It is also possible in some situations when fixed points are present. (Sec. 7.)

A Flowbox is the image of a piece of a transverse section isomorphic to a disk (the inset) translated using the flow onto another transverse section (the outset). See Fig. 3.1.

A Flowbox Covering is a set of flow boxes such that every point on M lies in at least one flow box.

A Flowbox Tiling is a set of flow boxes such that every point on M lies in one and only one flow box.

The flow box theorem [1] states that a flow box can be mapped to a coordinate system where the trajectories are straight. Each point in the flow box lies on a trajectory which passes through a point on the inset. The mapping which straightens the flow box uses the coordinates of this point on the inset and time.

3.2. Covering $M(\lambda)$ with flow boxes. We use flow boxes whose insets are balls in a plane orthogonal to a central trajectory fragment $\mathbf{u}_i(t)$, $t \in [0, \tau_i]$. By augmenting the central trajectory with the tangent space and a radius R (a “fat” trajectory [21], Fig. 3.4) a set of trajectory fragments which covers M well can be found. The radius controls the density and distribution of the fragments.

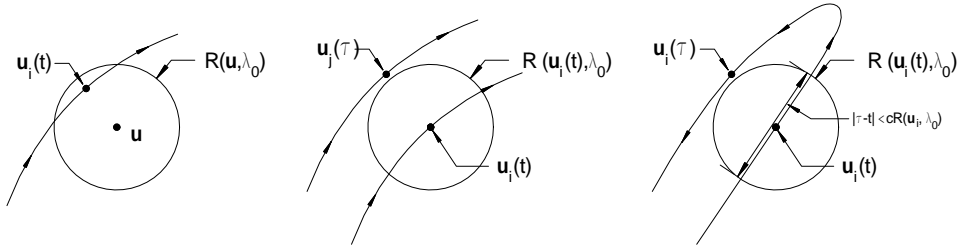


FIG. 3.2. l) Every point on M must be close to fragment of a trajectory. c) Two trajectory fragments cannot be too close to one another. r) A fragment cannot come back too close to itself.

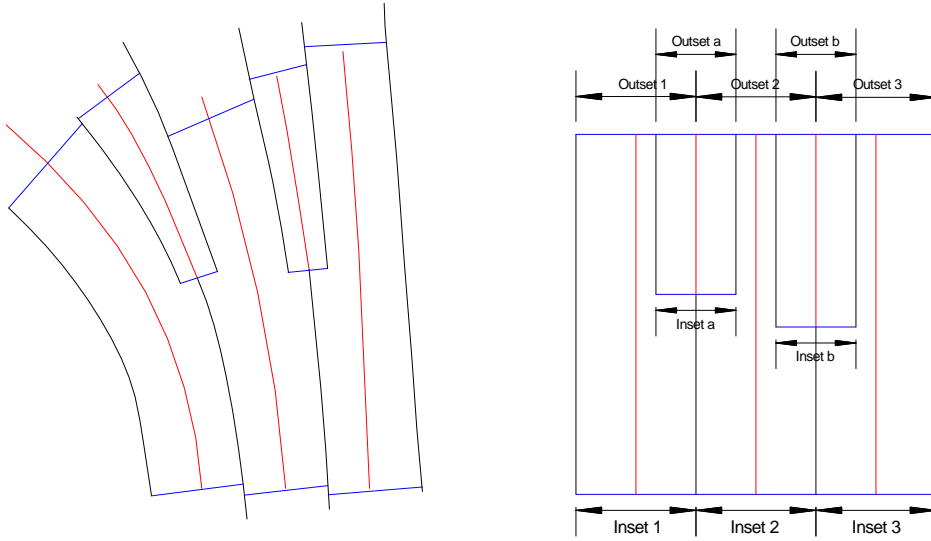


FIG. 3.3. (l) A pair of adjacent flow boxes in a two dimensional flow. The width of the boxes increases, and at some point a third box is inserted. (r) The same flow boxes in straightened coordinates, showing the construction of a tiling from the covering.

A set of trajectories covers M well if

- a) **Minimum Density:** For every $\mathbf{u} \in M(\lambda)$, there is a point on a trajectory fragment $\mathbf{u}_i(t)$ at some $t \in [0, T_i]$, such that

$$|\mathbf{u} - \mathbf{u}_i(t)| \leq R(\mathbf{u}, \lambda).$$

- b) **Maximum Density I.:** For every pair of points on two different fragments $\mathbf{u}_i(t)$, $t \in [0, T_i]$ and $\mathbf{u}_j(\tau)$, $\tau \in [0, T_j]$, with $i < j$

$$|\mathbf{u}_i(t) - \mathbf{u}_j(\tau)| \geq R(\mathbf{u}_i(t), \lambda).$$

- c) **Maximum Density II.:** For every pair of points on the same fragment, $\mathbf{u}_i(t)$, $t \in [0, T_i]$ and $\mathbf{u}_i(\tau)$, $\tau \in [0, T_i]$ there is a constant $C > 0$ such that if

$$|\mathbf{u}_i(t) - \mathbf{u}_i(\tau)| \leq R(\mathbf{u}_i(t), \lambda)$$

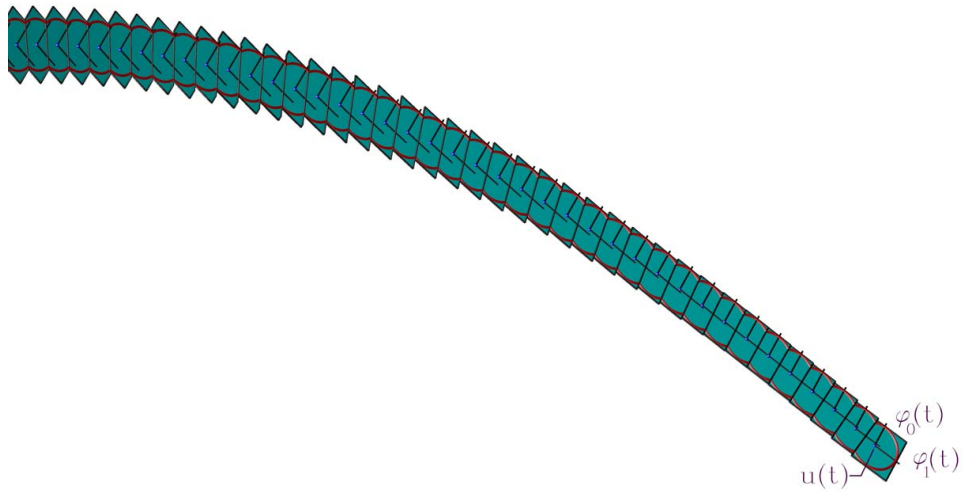


FIG. 3.4. A “fat” trajectory

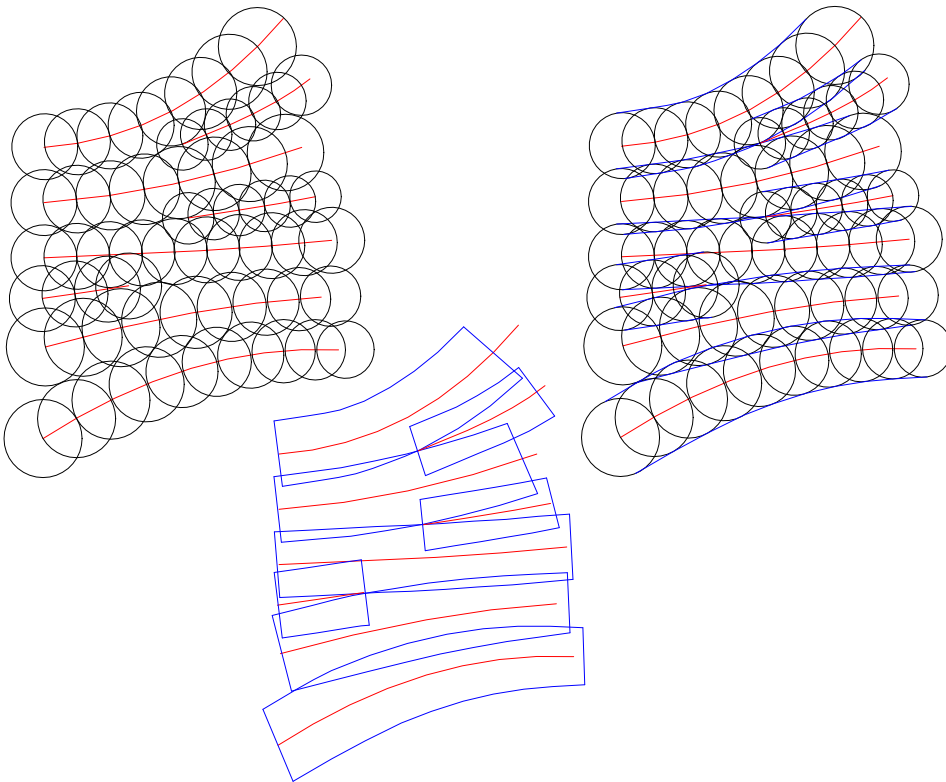


FIG. 3.5. l) Part of a covering of the plane by fat trajectories. c) The envelopes of the balls along the fat trajectories. r) Overlapping flowboxes constructed by modifying the envelopes.

then

$$|t - \tau| \leq CR(\mathbf{u}(t), \lambda).$$

To construct the trajectory fragments an initial point is used to integrate a fat trajectory until it returns into one of the balls. If a parametric form exists for the initial guess then an initial points on M are easily obtained, and if a global transversal exists and is known initial points may be drawn from the transversal. This process is repeated until there are no more initial points available. It was shown in [20] and [21] how to obtain an initial point which either maximizes the outward flow from the boundary of the collection of balls, or if no such point exists to obtain a point on the boundary. Since M is closed this process must terminate if the radius is bounded away from zero. This approach was used to construct the covering shown in Fig. 3.6, which is close to a quasiperiodic torus, which has a closed global transversal.

A Fat Trajectory $(\mathbf{u}(t), \Phi(t), R(t))$ is a quadratic approximation

$$v^i(t, s) = u^i(t) + \sum_p \Phi_p^i(t) s^p + \frac{1}{2} \sum_{p,q} A_{pq}^i(t) s^p s^q + O(|s|^3)$$

to a k -dimensional manifold on a trajectory $\mathbf{u}(t)$, with tangent space spanned by the k orthonormal columns of $\Phi(t)$. The radius $R(t)$ is chosen small enough that for some small ϵ , which is an accuracy parameter –

$$(3.1) \quad \frac{1}{2} |A_{jk}^i(t)| R^2(t) \leq \epsilon \quad \longrightarrow \quad R(t) \leq \sqrt{\frac{2\epsilon}{|A_{jk}^i(t)|}}.$$

This relates the radius $R(t)$ to the maximum distance ϵ between the tangent space and the manifold (measured orthogonal to the tangent space) and the minimum curvature $|A_{jk}^i(t)|$. It was shown in [21] that the orthonormal basis evolves according to the flow

$$(3.2) \quad \frac{\partial}{\partial t} \Phi_j^i(t) = \sum_p f_{,p}^i \Phi_j^p - \sum_{p,q} \Phi_r^p \frac{\partial f^p}{\partial u^q} \Phi_j^q \Phi_r^i$$

An evolution equation can also be written for $A_{jk}^i(t)$.

A cylindrical tube exists along the fat trajectory. Rewriting Eq. 3.1 for $\mathbf{u} \in M$ near $\mathbf{u}(t)$ we have

$$|\Phi^T(t)(\mathbf{u} - \mathbf{u}(t))| < R(t) \quad \longrightarrow \quad |(I - \Phi(t)\Phi^T(t))(\mathbf{u} - \mathbf{u}(t))| < \epsilon$$

A flow box covering may be constructed from a fat trajectory covering of M . We have the cylinder defined by the envelope of the balls along the fat trajectory, and a flow box which has the ball at the beginning of the fat trajectory as inset. This flow box may not lie outside the cylinder along the entire fat trajectory fragment. If it does not, the radius of the inset may be increased until this requirement is met. Since the cylinders cover M the flow boxes must also cover M (Fig. 3.5.)

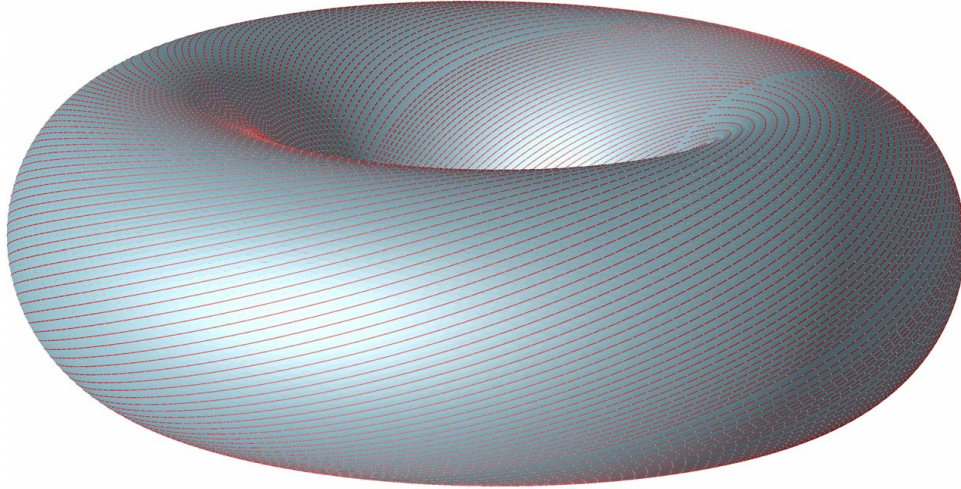


FIG. 3.6. A computed fat trajectory covering of the torus described in section 5. For this covering there are 182 trajectories. The longest has 223 points, and the shortest has 4 points. There are a total of 22,907 points.

3.3. Constructing a flow box tiling from a flow box covering. The following discussion is intended to motivate the formulation presented in the following sections. While the construction of a tiling from a covering is possible, it is unnecessary and likely to be computationally expensive.

Suppose that at a particular set of parameter value a compact invariant manifold $M(\lambda)$ exists and that there is a flow box covering of $M(\lambda)$. The sides of the flow boxes (excepting the inset and outset) consist of groups of trajectories, and can be quite complicated. Rather than trying to explicitly represent these boundaries to build a tiling, we use the Flowbox Theorem to map of the flow in the neighborhood of a trajectory to a parallel flow, and use for the boundary of the overlapping flow boxes cylinders about a “centerline” trajectory. The set of centerline trajectories make a set of trajectory fragments on M , and we will represent the flow box tiling by these fragments.

In principle a flow box tiling of $M(\lambda)$ may be found from these tubular neighborhoods of trajectory fragments. Choose one such flow box. The flow in a neighborhood of the center trajectory can be mapped to a parallel flow. The tubular neighborhoods become cylindrical neighborhoods. Using the same idea as in [20], but for cylinders instead of spherical balls, each pair of cylinders is partitioned into pieces by the plane containing the intersection of the cylinders. These pieces either lie entirely inside the union of the pair of cylinders or entirely outside. If this process is repeated for each tubular neighborhood which overlaps the chosen flowbox, and the overlapping portions of the flowbox have removed, what results is a tiling, and in the rectified coordinates the insets and outset are polyhedral. See Figs. 3.7 and 3.8.

An important feature of this construction (which we will not perform explicitly) is that the center trajectory is inside the truncated flowbox if the ratio of the radii of overlapping tubular neighborhoods is in the interval $[1/\sqrt{2}, \sqrt{2}]$.

3.4. Constructing a global section from a flow box tiling. Since tiled flow boxes are disjoint the outset cannot lie inside another flow box, and so must lie on

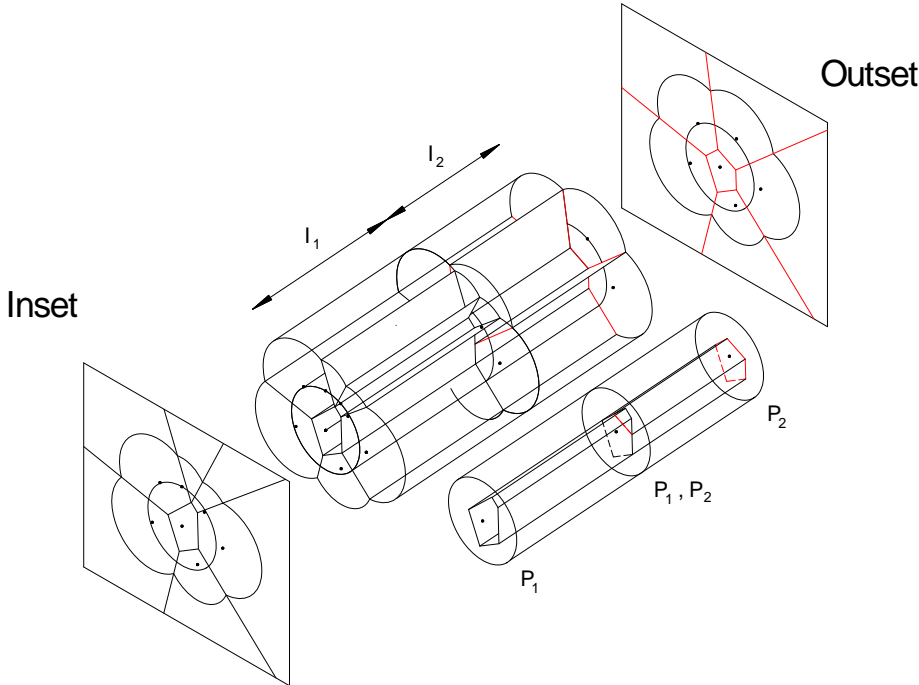


FIG. 3.7. A set of adjacent cylindrical flow boxes in a three dimensional flow in straightened coordinates, showing the construction of a tiling from the covering.

a subset of the insets. If the flow is smooth, this composite mapping is a piecewise smooth mapping from the union of all the insets to itself. If the insets are extended a small distance orthogonal to M the extended insets are transverse to M , and the intersection of M and the extended insets (the original set of insets), is a global section for the flow on M . (See Fig. 3.9.)

4. A system of coupled two point boundary value problems approximating $M(\lambda + \Delta\lambda)$. To find $M(\lambda + \Delta\lambda)$ from $M(\lambda)$ we proceed in much the same way as for periodic orbits. We use the extended insets from $M(\lambda)$ and perturb the flow. Instead of constructing the mapping between the extended insets, and then finding a set of invariant curves of the map we will find a set of trajectory fragments on $M(\lambda + \Delta\lambda)$ which serve as centerline trajectories for a new set of covering flow boxes for $M(\lambda + \Delta\lambda)$.

The set of initial points $\mathbf{u}_i(0) \in M(\lambda)$ and fragment lengths $\tau_i > 0$ uniquely define the set of trajectory fragments on $M(\lambda)$. Let \mathbf{v}_i and $\hat{\tau}_i$ be the corresponding set of fragments on the perturbed manifold $M(\lambda + \Delta\lambda)$. To determine $\mathbf{v}_i(0) \in M(\lambda + \Delta\lambda)$ and $\hat{\tau}_i$ we pose an initial value problem with a set of n (the dimension of points on M) algebraic constraints and one integral phase condition. The first k algebraic equations fix the projection of $\mathbf{v}_i(0)$ onto $\Phi(\mathbf{u}_i(0))$, the tangent space of $M(\lambda)$ at $\mathbf{u}_i(0)$. In addition $\mathbf{v}_i(1) - \mathbf{u}_i(1)$ must lie in the orthogonal complement of the flow at $\mathbf{u}_i(1)$, and $\mathbf{v}_i(1)$ must lie on $M(\lambda + \Delta\lambda)$. Since $M(\lambda + \Delta\lambda)$ is unknown, we instead approximate this $M(\lambda + \Delta\lambda)$ using interpolation between nearby trajectory fragments.

We assume that $\Delta\lambda$ small enough so that $M(\lambda + \Delta\lambda)$ is a graph $\mathbf{a}_i(\mathbf{u}, \mathbf{s})$ on $\Phi(\mathbf{u}, \lambda)$ in a neighborhood of \mathbf{u} .

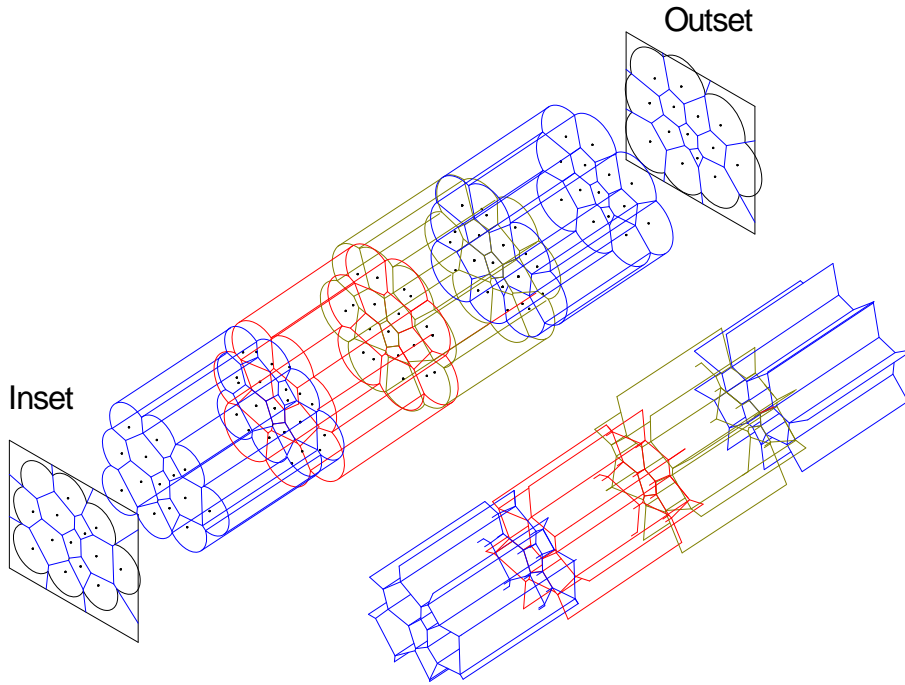


FIG. 3.8. Continuing the construction in the previous figure. The mapping from the inset to the outset can be seen to be (in the straightened flow) a mapping from a polygonal (polyhedral) tiling of the inset to a tiling of the outset.

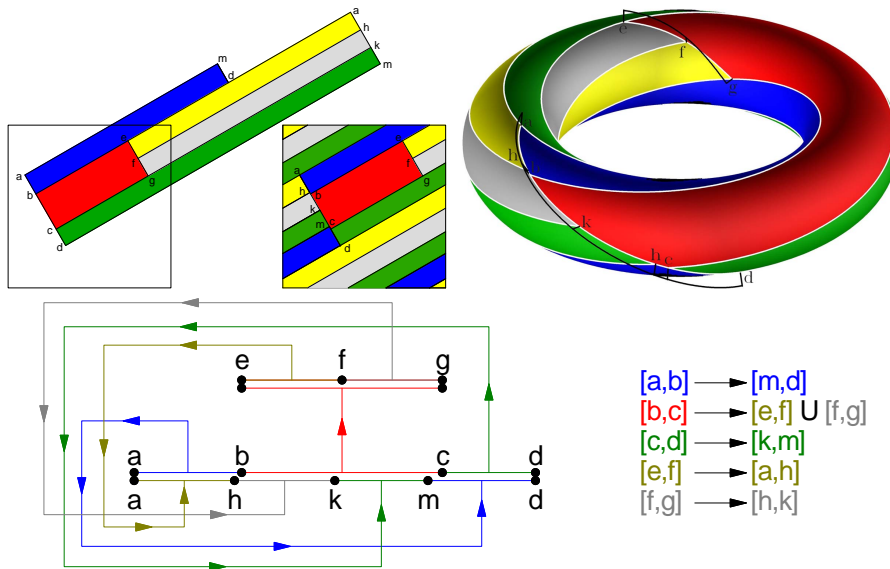


FIG. 3.9. (l) A tiling of an invariant torus with flow boxes. (l) in the periodic domain., (r) In three dimensions, with outsets extended off the torus. (b) the corresponding interval map.

For $\mathbf{s}_i(t) \in \mathbb{R}^k$, $|\mathbf{s}_i(t)| \leq R(t)$,

$$\mathbf{v}_i(t) = \mathbf{u}_i(t) + \Phi(\mathbf{u}_i(t))\mathbf{s}_i(t) + \mathbf{a}_i(\mathbf{u}_i(t), \mathbf{s}_i(t)),$$

$$\Phi^T(\mathbf{u}_i(t))\mathbf{a}_i(\mathbf{u}_i(t), \mathbf{s}_i(t)) = 0,$$

$$\Rightarrow \quad \mathbf{s}_i(t) = \Phi^T(\mathbf{u}_i(t))(\mathbf{v}_i(t) - \mathbf{u}_i(t)).$$

The trajectory $\mathbf{v}_i(t)$ must lie on $M(\lambda + \Delta\lambda)$, but its length $\hat{\tau}_i$ and projection onto $M(\lambda)$ are undetermined.

One choice is to require that the projection of the initial point $\mathbf{v}_i(0)$ is $\mathbf{u}_i(0)$:

$$\mathbf{s}_i(0) = \Phi_i^T(\mathbf{u}_i(0))(\mathbf{v}_i(0) - \mathbf{u}_i(0)) = 0.$$

The length of the trajectory fragment can be fixed by requiring that $\mathbf{v}(1)$ lie on a section through $\mathbf{u}_i(1)$ orthogonal the flow:

$$\mathbf{f}_i^T(\mathbf{u}_i(1))(\mathbf{v}_i(1) - \mathbf{u}_i(1)) = 0.$$

This results in the following TPBVP for $\mathbf{v}_i(t)$:

$$\begin{aligned} \mathbf{v}_i'(t) &= \hat{\tau}_i \mathbf{f}(\mathbf{v}_i(t), \lambda + \Delta\lambda) & t \in [0, 1] \\ \Phi^T(\mathbf{u}_i(0))(\mathbf{v}_i(0) - \mathbf{u}_i(0)) &= 0, \\ \mathbf{f}^T(\mathbf{u}_i(1))(\mathbf{v}_i(1) - \mathbf{u}_i(1)) &= 0, \\ [I - \Phi(\mathbf{u}_i(1))\Phi^T(\mathbf{u}_i(1))] &(\mathbf{v}_i(1) - \mathbf{u}_i(1)) = \mathbf{a}_i(\mathbf{u}_i(1), \mathbf{s}) \end{aligned} \tag{4.1}$$

where $\mathbf{s} = \Phi^T(\mathbf{u}_i(1))(\mathbf{v}_i(1) - \mathbf{u}_i(1))$. The graph $\mathbf{a}_i(\mathbf{u}_i(1), \mathbf{s})$ is of course not known. Below we discuss how to approximate \mathbf{a}_i by interpolating between nearby trajectories.

For periodic solutions an integral phase condition performs much better than a simple end condition. Given the similarities we therefor replace the second boundary condition in Eq. 4.1 with an integral phase condition

$$\int_0^1 \mathbf{f}^T(\mathbf{u}_i(t), \lambda)(\mathbf{v}_i(t) - \mathbf{u}_i(t)) dt = 0.$$

This determines $\hat{\tau}_i$ so that the correspondance in t between the two fragments is as close as possible. The analogy to the invariant curve algorithms is lost, since there is no fixed end section, but the the third condition in Eq. 4.1 remains unchanged, except that $\mathbf{s}_i(1)$ can lie in the full tangent space.

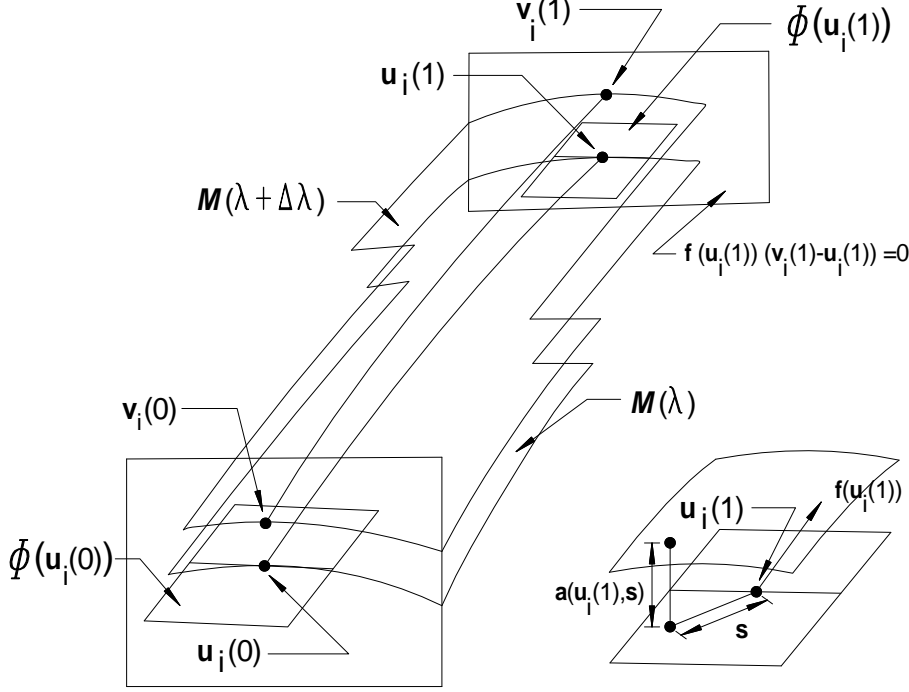


FIG. 4.1. A trajectory fragment on $M(\lambda + \Delta\lambda)$ and its relation (through the two point boundary value problem) to the corresponding fragment on $M(\lambda)$. The boundary conditions are on the left: $\mathbf{v}_i(0)$ projects onto $\mathbf{u}_i(0)$, and on the right: $\mathbf{v}_i(1)$ lies in Σ , and on $\mathbf{v}(\mathbf{s})$, where \mathbf{s} is the orthogonal projection of $\mathbf{v}_i(1)$ onto the tangent space $\Phi(\mathbf{u}_i(1))$ at λ

The final TPBVP is (Fig. 4.1.)

$$\mathbf{v}'_i(t) = \hat{\tau}_i \mathbf{f}(\mathbf{v}_i(t), \lambda + \Delta\lambda) \quad t \in [0, 1]$$

$$\text{with} \quad \mathbf{s}_i(t) = \Phi^T(\mathbf{u}_i(t)) (\mathbf{v}_i(t) - \mathbf{u}_i(t)),$$

(4.2)

$$k \quad \Phi^T(\mathbf{u}_i(0)) (\mathbf{v}_i(0) - \mathbf{u}_i(0)) = 0$$

$$n - k \quad [I - \Phi(\mathbf{u}_i(1))\Phi^T(\mathbf{u}_i(1))] (\mathbf{v}_i(1) - \mathbf{u}_i(1)) = \mathbf{a}_i(\mathbf{u}_i(1), \mathbf{s}_i(1))$$

$$1 \quad \int_0^1 \mathbf{f}^T(\mathbf{u}_i(t), \lambda) (\mathbf{v}_i(t) - \mathbf{u}_i(t)) dt = 0.$$

4.1. Interpolation. Since $\mathbf{a}_i(\mathbf{u}_i(t), \mathbf{s})$ is not known, it must be approximated. We have a distribution of points on M , so it is natural to use an interpolation using nearby values of \mathbf{v} . This requires that $M(\lambda + \Delta\lambda)$ have a certain smoothness. Without smoothness beyond some scale there is little hope of computing M , so this is not an unreasonable assumption. If $\mathbf{u}_j(t_j)$, $j \in J_i$ are a set of points near $\mathbf{u}_i(1)$, then

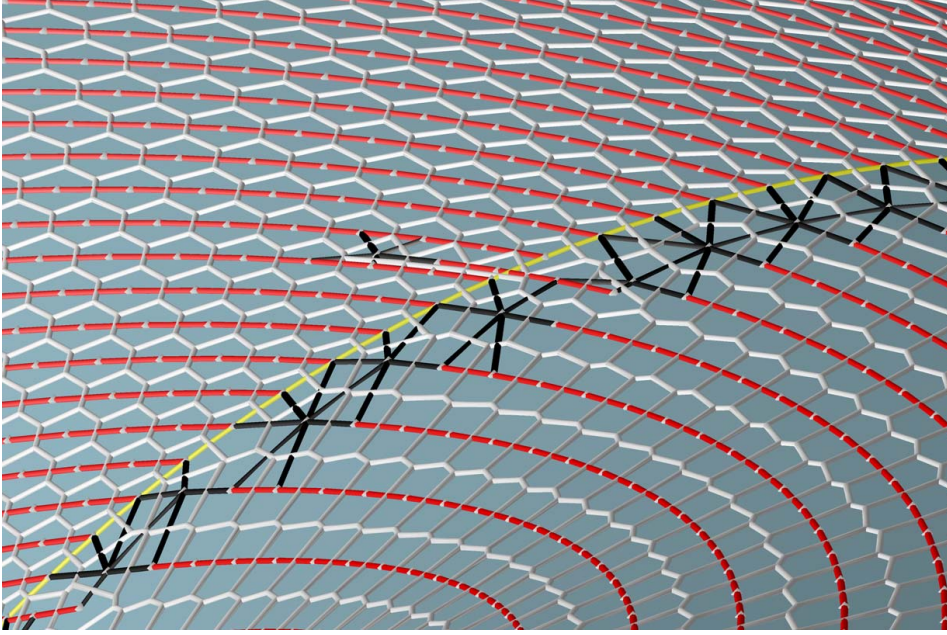


FIG. 4.2. Nearest neighbors of trajectory ends in the covering of the torus described in section 5 and shown in Fig. 3.6.

interpolants are usually of the form

$$\begin{aligned} \mathbf{a}_i(\mathbf{u}_i(1), \mathbf{s}) &= \sum_j \alpha_j(\mathbf{s}) \mathbf{a}_i(\mathbf{u}_i(1), \mathbf{s}_j(t_j)) \\ &= \sum_j \alpha_j(\mathbf{s}) [I - \Phi(\mathbf{u}_i(1))\Phi^T(\mathbf{u}_i(1))] (\mathbf{v}_j(t_j) - \mathbf{u}_i(1)) \end{aligned}$$

The $\alpha_j(\mathbf{s})$'s are interpolation weights assigned to each $\mathbf{v}_j(t_j)$, with $\sum_j \alpha_j(\mathbf{s}) = 1$. The accuracy of the interpolation depends on the curvature of $M(\lambda)$ at \mathbf{u} , the width and geometric arrangement of the “stencil” $\{\mathbf{u}_j(t_j)\}$. Fig. 4.2 shows the stencils for a few of the trajectories of the tiling shown in Fig. 3.6.

Several choices are available for interpolation on triangulations. Fig. 4.3 is a sketch of Sibson's method [31] which is implemented in CGAL [10]. Sibson's method constructs two Voronoi diagrams of the interior of the convexhull of the $\mathbf{s}_j(t_j)$. One diagram excludes $\mathbf{s}_i(1)$, and the cell associated with $\mathbf{s}_j(t_j)$ we will call V_j . The second diagram includes $\mathbf{s}_i(1)$ and the cell associated with $\mathbf{s}_j(t_j)$ will be W_j and the cell of $\mathbf{s}_i(1)$ will be W_i . Then the weights are (Fig. 4.3)

$$\alpha_j = \frac{\text{vol}(W_i \cap V_j)}{\sum_j \text{vol}(W_i \cap V_j)}$$

Other “natural neighbor” interpolants are discussed in [8]. These interpolants are smooth within the convex hull of the neighbors, but only C^1 over a Delaunay triangulation of the points. Interpolants with higher degrees of smoothness can be found in [16].

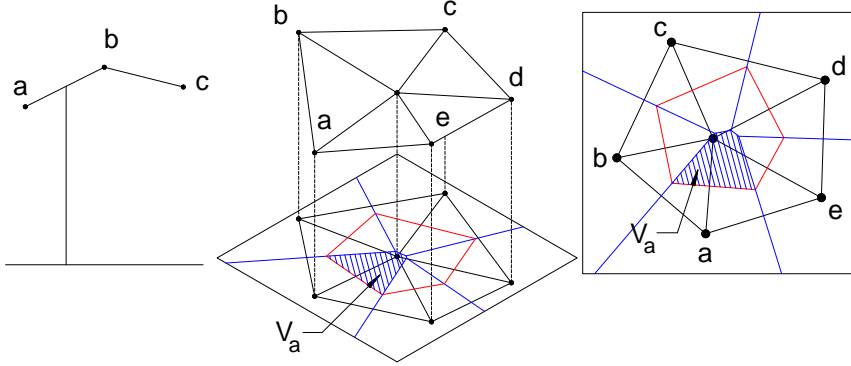


FIG. 4.3. A sketch of Sibson's natural neighbor interpolation. Each vertex **a-e** has a Voronoi cell without the point to be interpolated. If the volume of these individual cells within the convex hull of neighbors are V_a etc., the weight of point **a** in the interpolation is $V_a/(V_a + V_b + V_c + \dots)$.

4.2. Solution Methods. The system posed for the invariant manifold is a set of coupled TPBVP's it is natural to use a continuation method based on collocation methods (AUTO [13] or COLSYS [4]). to track the changes in the manifold. Note however that the boundary conditions may involve points which are interior to the trajectory fragment, or to adjacent fragments. Therefore boundary conditions of the form $bc(\mathbf{u}(\mathbf{0}), \mathbf{u}(1), \lambda) = 0$ will not suffice. Both AUTO and COLSYS use a condensation of parameters and nested dissection to solve the bordered linear systems (Fig. 4.4) to implement Newton's method for solving the nonlinear system. We would prefer not to destroy this structure. As written the system for the invariant manifold has a Jacobian with the structure shown in Fig. 4.5. A rearrangement which gathers the lengths τ_i of the fragments with the parameters λ and the boundary conditions with the arclength constraints (Fig. 4.6 almost recovers the structure of the original system. This is equivalent to casting the TPBVP's for the fragments as a TPBVP for a vector which is the concatenation $(\mathbf{u}_0, \mathbf{u}_1, \dots, \mathbf{u}_{n-2}, \mathbf{u}_{n-1})$. The only modification required is that the coupling of the interpolation of the right hand boundary conditions. This means that those boundary conditions become sparse rows in the Jacobian, much like integral constraints or the arclength constraints. In addition shorter trajectories require fewer points than longer ones, and solvers assume that all component TPBVPs have the same discretization.

4.3. Making a step. In order to make a continuation step we need to obtain the same information we had for $M(\lambda)$. That is, we need a set of well spaced trajectory fragments and tangent spaces at $t = 1$ for each fragment. The solution of the TPBVP gives a set of trajectory fragments, and the tangent space at $t = 1$ can be found from the interpolant which was used for the boundary condition at $t = 1$. Some fragments are likely to become too close together and others too far apart. We use fat trajectories again to create a new covering. This time however, the trajectory is known, so only the flow for the tangentspace is needed, and we integrate backward in time, since the tangent space is estimated at $t = 1$.

To eliminate trajectories that are too close together one may step along each trajectory in turn and end trajectories which come too close. At the same time, since curvatures will have changed, the size of the balls along the trajectories need to be adjusted, and new balls inserted or removed from the trajectory to ensure that the

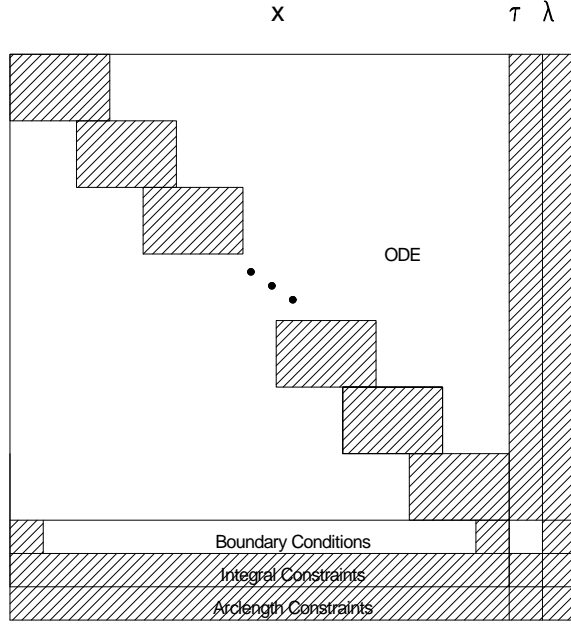


FIG. 4.4. The layout of the Jacobian in AUTO's formulation of a TPBVP.

trajectory is covered once the radii are adjusted. These two procedures, and the movement of trajectories away from each other, will open gaps in the ball covering of $M(\lambda + \Delta)$. Identifying interpolation points and creating new fat trajectories will close these gaps and the algorithm may continue.

5. A partial example – an invariant torus. As an example we compute an invariant torus in a simple system from [3]. The system is

$$\begin{aligned}
 x'_0 &= x_0 + 0.55y_0 - (x_0^2 + y_0^2)x_0 - \lambda(x_0 + y_0 - x_1 - y_1) \\
 y'_0 &= -0.55x_0 + y_0 - (x_0^2 + y_0^2)y_0 - \lambda(x_0 + y_0 - x_1 - y_1) \\
 x'_1 &= x_1 + 0.55y_1 - (x_1^2 + y_1^2)x_1 + \lambda(x_0 + y_0 - x_1 - y_1) \\
 y'_1 &= -0.55x_1 + y_1 - (x_1^2 + y_1^2)y_1 + \lambda(x_0 + y_0 - x_1 - y_1)
 \end{aligned}$$

This system is a pair of coupled nonlinear oscillators, with λ controlling the strength of the coupling. This gives us the initial invariant torus, at $\lambda = 0$, which is the product of the two oscillatory motions. As λ increases the torus develops sharp folds, which with other methods require some kind of adaptive meshing.

A covering for the invariant torus at $\lambda = 0.05$ is shown in Fig. 3.6. As an example of the TPBVP's, for trajectory fragment 76 the right end boundary condition depends on the points

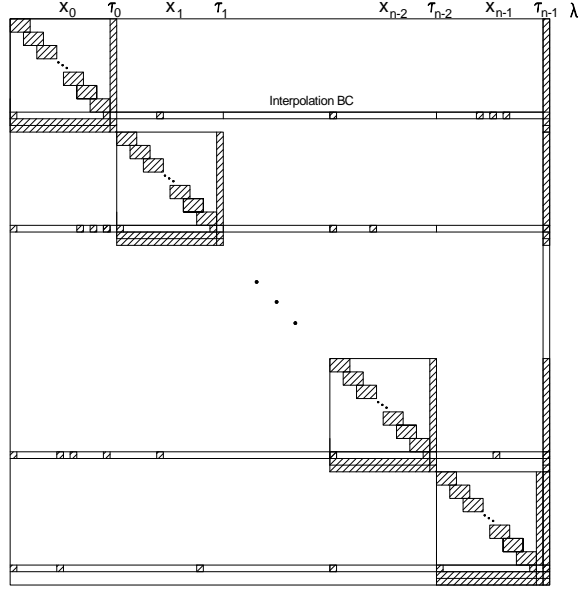


FIG. 4.5. The layout of the Jacobian in AUTO's formulation of the trajectory fragments in the system for the invariant manifold.

Trajectory 76				
	x_0	y_0	x_1	y_1
$u_{76}(0.000000)$	0.984153	0.000000	0.046339	1.002124
ϕ_0	-0.039520	0.000000	-0.997967	0.050006
ϕ_1	(0.023109	-0.999631	-0.001625	-0.014176
$u_{76}(1.000000)$	1.003289	0.037685	0.802945	0.586386
ϕ_0	0.010329	-0.291224	-0.559801	0.775684
ϕ_1	0.050356	-0.955017	0.151557	-0.249859

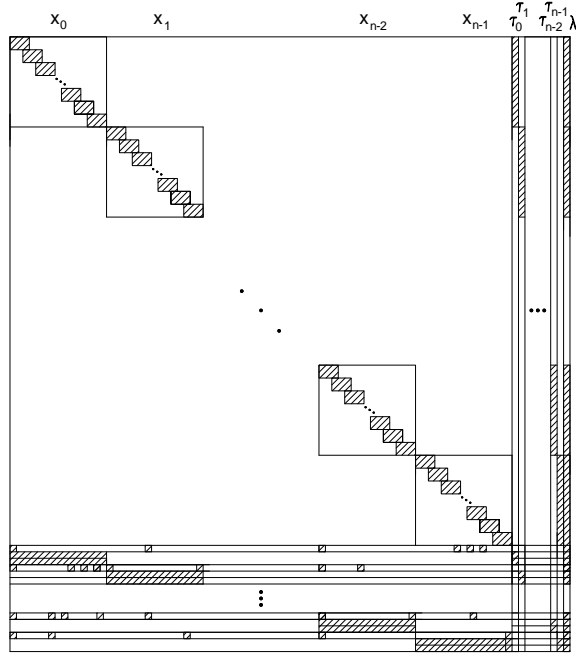


FIG. 4.6. A rearrangement of the Jacobian in AUTO's formulation of the trajectory fragments in the system for the invariant manifold.

	x_0	y_0	x_1	y_1
$u_{30}(0.000000)$	1.004652	0.000000	0.818318	0.563085
ϕ_0	-0.003910	0.000000	-0.566333	0.824167
ϕ_1	0.013697	-0.999626	-0.019544	-0.013365
$u_{32}(0.000000)$	1.004465	0.000000	0.795029	0.595615
ϕ_0	-0.005445	0.000000	-0.597650	0.801738
ϕ_1	0.013730	-0.999625	-0.019030	-0.014093
$u_{70}(1.000000)$	1.002803	0.049669	0.832593	0.543868
ϕ_0	0.014661	-0.271879	-0.522082	0.808253
ϕ_1	0.061428	-0.960005	0.128701	-0.240923
$u_{70}(0.995586)$	1.000464	0.078529	0.816493	0.568841
ϕ_0	0.021212	-0.270781	-0.545275	0.793019
ϕ_1	0.089121	-0.958049	0.136207	-0.235877
$u_{76}(0.995613)$	1.001234	0.066518	0.785648	0.610509
ϕ_0	0.017415	-0.290159	-0.582060	0.759402
ϕ_1	0.077962	-0.953416	0.159228	-0.244046
$u_{80}(1.000000)$	1.002366	0.047948	0.768485	0.631512
ϕ_0	0.011733	-0.302262	-0.600193	0.740440
ϕ_1	0.060623	-0.950992	0.172546	-0.249319

For this covering there were 182 trajectories. The longest had 223 points, and the shortest had 4 points. There were a total of 22,907 points. So the linear system is size $22,907 + 182 + 1 = 23,090$, with 182 blocks ranging in size from 2×4 to 221×223 with $2 \times 182 + 1 = 364$ "full" rows (which are quite sparse) for the boundary conditions

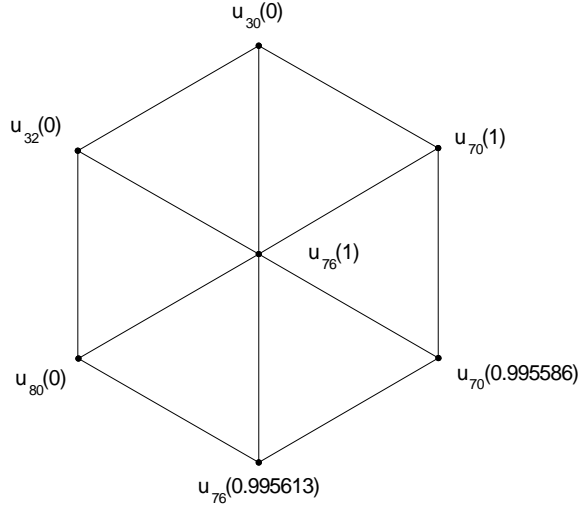


FIG. 5.1. The support for the interpolation boundary condition for trajectory 76. The positions shown do not reflect the actual relative positions of the points.

and pseudo-arclength constraint.

6. Summary. The algorithm described in this paper represents a compact invariant manifold $M(\lambda)$ as the solution of a system of coupled TPBVPs. A fat trajectory covering of $M(\lambda)$, if it exists, implies that there is a flow box covering of $M(\lambda)$. The flow box covering in turn generates a flow box tiling of $M(\lambda)$, which is associated with a piecewise smooth return map from the set of insets of the tiling to itself. Instead of finding invariant curves of this return map we find a single point on the inset of each flow box tile. The mapping of the point to the outset of the tile is a TPBVP, and if an interpolation is used to approximate the invariant set of the return map we arrive at the system of coupled TPBVPs.

There are of course parallels to existing methods. Interpolation boundary conditions are used for finding invariant circles for invariant quasiperiodic tori [32]. The system of coupled TPBVPs may also be interpreted as a characteristic of a PDE on a complicated domain (“Manhattan Towers” [5]).

The flowbox tiling provides a natural approach to generating a quality mesh on the manifold. This mesh has the benefit that the mesh lines are trajectories, and the linear system which results can be reduced in size by elimination along the trajectories. This is roughly equivalent to the construction of the return map.

Beyond the construction of the initial covering and posing of the system of the two point boundary value problems (TPBVPs), this algorithm has not yet been implemented. Although the system is similar to the form usually used for TPBVPs there are significant differences that appear to prevent any existing code for TPBVPs being used. The system may be posed as a single TPBVP, in the example of Sec. 5 this would be a first order ODE for points $\mathbf{u} \in \mathbb{R}^{4 \times 182}$, but the boundary conditions are not functions just of $\mathbf{u}(0)$ and $\mathbf{u}(1)$, they involve values at various interior points as well. In addition, the mesh on each ODE should be different - the difference in length of the trajectory fragments can be significant and the required points for interpolation need to be included in the meshes. The author is not aware of any package that will handle these two requirements, although the techniques used by collocation codes

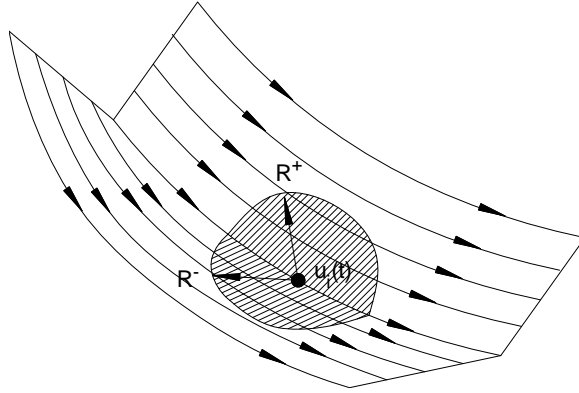


FIG. 7.1. A discontinuity in derivative propagating along a trajectory, and one of the two associated balls.

such as AUTO and COLNEW could be easily modified.

7. Extensions. No constraint has been placed on the smoothness of $M(\lambda)$, although we need at least continuity. Discontinuities in derivatives propagate along trajectories, so that the set of such singular points on $M(\lambda)$ form an a set of invariant manifolds. We will require that these be a finite number of these singular invariant sub-manifolds, that they be co-dimension 1 on $M(\lambda)$, and that they have finite volume. The assumptions listed above involving spherical neighborhoods are generalized so that on each singular invariant sub-manifold there are two radii functions R_i^+ and R_i^- , and instead of using spherical neighborhoods for the constraints on closeness and minimal separation, two half spherical neighborhoods are used, each on the appropriate side of the invariant sub-manifold (this is the motivation of the requirement that they be co-dimension one). With these generalizations, and a covering of the sub-manifolds by trajectories exactly like the covering of $M(\lambda)$ the following arguments and algorithms apply.

If a ball is placed about each fixed point, and all fixed points are hyperbolic, then the surface of the ball can be decomposed into subsurfaces which are transverse to the flow and bounded by the codimension 1 curves where the flow is tangent to the surface of the ball and the intersections of the surface and the stable and unstable manifolds of the fixed point.

REFERENCES

- [1] R. ABRAHAM AND J. E. MARSDEN, *Foundations of Mechanics*, Addison Wesley, Reading, MA, 1978.
- [2] E. L. ALLGOWER AND K. GEORG, *Introduction to Numerical Continuation Methods*, Classics in Applied Mathematics, SIAM, Philadelphia, 2003.
- [3] D. G. ARONSON, E. J. DOEDEL, AND H. G. OTHMER, *The dynamics of coupled current-biased Josephson junctions - part II*, International journal of bifurcation and chaos, 1 (1991), pp. 51–66.
- [4] U. ASCHER, J. CHRISTIANSEN, AND R. D. RUSSELL, *Collocation software for boundary-value odes*, ACM Transactions on Mathematical Software, 7 (1981), pp. 209–222.
- [5] W. BASENER, *Every nonsingular C^1 flow on a closed manifold of dimension greater than two has a global transverse disk*, Topology and its Applications, 135 (2004), pp. 131–148.
- [6] W.-J. BEYN, *The numerical computation of connecting orbits indynamical systems*, IMA J. Num. Anal., 9 (1990), pp. 379–405.

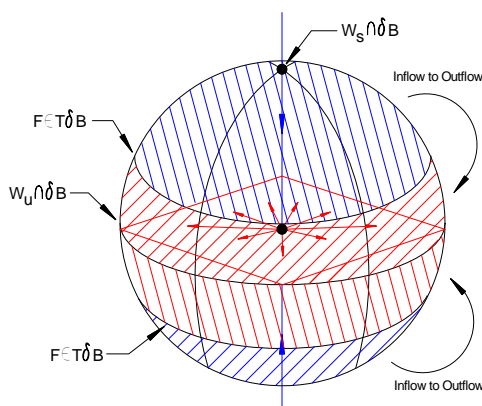


FIG. 7.2. A spherical ball placed around a hyperbolic singular with 1 dimension stable and 2 dimensional unstable manifolds.

- [7] G. D. BIRKHOFF, *Dynamical Systems*, no. 9 in Colloquium Publications, The American Mathematical Society, Providence, Rhode Island, 1927.
- [8] J.-D. BOSSONNAT AND F. CAZALS, *Smooth surface reconstruction via natural neighbor interpolation of distance functions*, *Computational Geometry*, 22 (2000), pp. 185 – 203.
- [9] H. W. BROER, H. M. OSINGA, AND G. VEGTER, *Algorithms for computing normally hyperbolic invariant manifolds*, *Z. angew. Math. Phys.*, 48 (1997), pp. 480–524.
- [10] CGAL, *Computational Geometry Algorithms Library*. <http://www.cgal.org>.
- [11] A. CHAMPNEYS, Y. A. KUZNETSOV, AND B. STANDSTEDT, *A numerical toolbox for homoclinic bifurcation analysis*, *International Journal on Bifurcation and Chaos*, 6 (1996), pp. 867–887.
- [12] L. DIECI AND J. LORENZ, *Computation of invariant tori by the method of characteristics*, *SIAM J. Numer. Anal.*, 32 (1995), pp. 1436–1474.
- [13] E. J. DOEDEL, *AUTO, a program for the automatic bifurcation analysis of autonomous systems*, *Cong. Numer.*, 30 (1981), pp. 265–384.
- [14] E. J. DOEDEL, H. B. KELLER, AND J. P. KERNÉVEZ, *Numerical analysis and control of bifurcation problems, part i: Bifurcation in finite dimensions*, *Int. J. Bifurcation and Chaos*, 1 (1991), pp. 493–520.
- [15] ———, *Numerical analysis and control of bifurcation problems, part ii: Bifurcation in infinite dimensions*, *Int. J. Bifurcation and Chaos*, 1 (1991), pp. 745–772.
- [16] G. E. FARIN, *Curves and surfaces for CAD: a practical guide*, Morgan-Kaufman, 2002.
- [17] N. FENICHEL, *Persistence and smoothness of invariant manifolds for flows*, *Indiana University Mathematics Journal*, 21 (1971), pp. 193–226.
- [18] M. J. FRIEDMAN AND E. J. DOEDEL, *Numerical computation and continuation of invariant manifolds connecting fixed points*, *SIAM J. Numer. Anal.*, 28 (1991), pp. 789–808.
- [19] W. J. F. GOVAERTS, *Numerical Methods for Bifurcations of Dynamical Equilibria*, SIAM, Philadelphia, 2000.
- [20] M. E. HENDERSON, *Multiple parameter continuation: Computing implicitly defined k -manifolds*, *International Journal of Bifurcation and Chaos*, 12 (2002), pp. 451–476.
- [21] ———, *Computing invariant manifolds by integrating fat trajectories*, *SIADS*, 4 (2005), pp. 832–882.
- [22] M. W. HIRSCH, C. PUGH, AND M. SHUB, *Invariant Manifolds*, vol. 253 of *Lecture Notes in Mathematics*, Springer, New York, 1977.
- [23] E. A. JACKSON, *Perspectives of Nonlinear Dynamics, Volume 1*, Cambridge University Press, Cambridge, 1990.
- [24] A. KATOK AND B. HASSELBLATT, *Introduction to the Modern Theory of Dynamical Systems*, Cambridge University Press, Cambridge, 1995.
- [25] B. KRAUSKOPF, H. OSINGA, E. DOEDEL, M. HENDERSON, J. GUCKENHEIMER, A. VLADIMIRSKY, M. DELLNITZ, AND O. JUNGE, *A survey of methods for computing (un)stable manifolds of vector fields*, *International Journal of Bifurcation and Chaos*, 15 (2005), pp. 2127–2143.
- [26] G. MOORE, *Computation and parameterization of invariant curves and tori*, *SIAM J. Numer. Anal.*, 33 (1996), pp. 2333–2358.
- [27] H. M. OSINGA, *Computing Invariant Manifolds, Variations on the Graph Transform*, PhD

- thesis, Rijksuniversiteit Groningen, June 1996.
- [28] B. RASSMUSSEN AND L. DIECI, *A geometrical method for the approximation of invariant tori*, Computational and Applied Mathematics, 216 (2008), pp. 388–412.
 - [29] V. REICHEL, *Computing invariant tori and circles in dynamical systems of fixed points*, in The IMA Volumes in Mathematics and its Applications Volume 119, E. Doedel and L. S. Tuckerman, eds., Springer-Verlag, 2000, pp. 407–437.
 - [30] F. SCHILDER, H. M. OSINGA, AND W. VOGT, *Continuation of quasi-periodic invariant tori*, SIAM J. Applied Dynamical Systems, 4 (2005), pp. 459–488.
 - [31] R. SIBSON, *A vector identity for the Dirichlet tessellation*, Mathematical Proceedings, Cambridge Philosophical Society, 87 (1980), pp. 151–155.
 - [32] M. VAN VELDHUIZEN, *A new algorithm for the numerical approximation of an invariant curve*, SIAM J. Sci. Stat. Comput., 8 (1987), pp. 951–962.
 - [33] S. WIGGINS, *Normally Hyperbolic Invariant Manifolds in Dynamical Systems*, vol. 105 of Applied Mathematical Sciences, Springer-Verlag, New York, 1994.